An Improved Method for the DCOPF With Losses

Brent Eldridge, *Student Member, IEEE*, Richard O'Neill, *Member, IEEE*, and Anya Castillo, *Member, IEEE*

***Abstract*—This paper discusses the marginal line loss approximation in the dc optimal power flow (DCOPF) and proposes a new methodology that improves the accuracy of current practices. In practice, the DCOPF solution may have significant differences compared to the ac base point that determines marginal losses, and this paper provides the only published example that illustrates this problem to our knowledge. The proposed methodology updates the marginal losses without solving a new ac base point so that the optimal solution accurately reflects system losses. Previously proposed methodologies require nonlinear programming solvers, additional ac power flow solutions, or are less accurate compared to actual losses, and they only give results for one or two test networks. This paper provides results on nine different test networks. The key advantage of the proposed methodology is that it can be easily integrated into current market software.**

***Index Terms*—DC optimal power flow (DCOPF), transmission losses, marginal pricing, linear approximation, iterative algorithms.**

NOMENCLATURE

Lowercase will denote scalar values, uppercase will denote vectors, and uppercase bold will denote matrices.

Sets

$\mathcal{K}$	Set of transmission lines, $\{1,\ldots,K\}$.
$\mathcal{K}(i)$	Subset of $\mathcal{K}$ connected to node i.
$\mathcal{N}$	Set of nodes or buses, $\{1,\ldots,N\}$.

Indices

h	Iteration index.
i,j,n,m	Nodes or bus indices, $i,j,n,m \in \mathcal{N}$.
k	Transmission line index, $k \in \mathcal{K}$.

Parameters

a_{ijk}	Transformer tap ratio on branch k from i to j.
b_k	Branch susceptance on branch k, $K \times 1$.
g_k	Branch conductance on branch k, $K \times 1$.
ℓ^0	Line loss function constant.
r_k	Resistance on branch k, $K \times 1$.
x_k	Reactance on branch k, $K \times 1$.
γ_k	Loss approximation second order coefficient, $K \times 1$.
η_k	Loss approximation range coefficient, $K \times 1$.
ξ_k	Loss approximation domain coefficient, $K \times 1$.
ω	Damping parameter.
$\mathbf{1}$	Vector of ones.
D	Loss distribution factors with elements d_i, $N \times 1$.
LF	Loss factors with elements ℓf_i, $N \times 1$.
P_d	Power demand with elements p_i^d, $N \times 1$.
$P_{\max}$	Maximum generator output, $N \times 1$.
$P_{\min}$	Minimum generator output, $N \times 1$.
$T_{\max}$	Transmission branch power flow limit, $K \times 1$.
U	Marginal reference bus withdrawal, $N \times 1$.
W	Weighting vector with elements w_i, $N \times 1$.
Φ	Vector of phase-shifting transformer angle changes with elements ϕ_{ijk} for branch k from i to j, $K \times 1$.
$\mathbf{A}$	Network incidence matrix, $K \times N$.
$\mathbf{B}$	Nodal susceptance matrix, $N \times N$.
$\mathbf{B_d}$	Diagonal branch susceptance matrix with elements b_{ijk} for branch k from i to j, $K \times K$.
$\mathbf{G_s}$	Diagonal shunt conductance matrix with elements g_i^{sh} for bus i, $N \times N$.
$\mathbf{H}$	Voltage angle sensitivity matrix, $N \times N$.
$\mathbf{H_b}$	Submatrix of power balance sensitivity bordered matrix inverse, $N \times N$.
$\mathbf{I}$	Identity matrix.
$\mathbf{L}$	Marginal loss matrix, $K \times N$.
$\mathbf{S}$	Power balance sensitivity matrix, $N \times N$.
$\mathbf{T}$	Power transfer distribution factor (PTDF) matrix with elements $t_{(ijk,n)}$, $K \times N$.
$\mathcal{L}$	Branch loss factor matrix, $K \times N$.

Variables

ℓ_k	Line losses on branch k.
ℓ	Total network real power losses.
P	Net injections with elements p_i, $N \times 1$.
P_g	Power generation injection with elements p_i^g, $N \times 1$.
P_t	Power flow vector with elements p_{ijk}, $K \times 1$.
V	Voltage magnitudes with elements v_i, $N \times 1$.
Θ	Voltage angles with elements θ_i, $N \times 1$.

Dual Variables

$\alpha_{\max}$	Dual variable to the max generation constraint, $N \times 1$.
$\alpha_{\min}$	Dual variable to the min generation constraint, $N \times 1$.
λ	Dual variable to the power balance constraint.
μ	Dual variable to the transmission constraint, $K \times 1$.
σ	Dual variable to the loss function constraint.
Λ	Vector of locational marginal prices (LMPs), $N \times 1$.

Manuscript received February 2, 2017; revised June 11, 2017 and September 12, 2017; accepted November 4, 2017. Date of publication November 24, 2017; date of current version June 18, 2018. This paper is an abridged version of a non-peer reviewed paper that is available online [1]. The views presented are the personal views of the authors and not the Federal Energy Regulatory Commission (FERC) or any of its Commissioners. Paper no. TPWRS-00155-2017. *(Corresponding author: Brent Eldridge)*

B. Eldridge is with the Johns Hopkins University, Baltimore, MD 21218 USA, and also with the Federal Energy Regulatory Commission, Washington, DC 20426 USA (e-mail: b.eldridge@jhu.edu).

R. P. O'Neill is with the Federal Energy Regulatory Commission, Washington, DC 20426 USA (e-mail: richard.oneill@ferc.gov).

A. Castillo is with Sandia National Laboratories, Albuquerque, NM 87185-1140 USA (e-mail: arcasti@sandia.gov).

Color versions of one or more of the figures in this paper are available online at http://ieeexplore.ieee.org.

Digital Object Identifier 10.1109/TPWRS.2017.2776081

Functions

$c(\cdot)$ Monotonically increasing cost function.
$\circ$ Hadamard product.
$^\top$ Matrix or vector transpose.
$\sim$ Connected to.

I. Introduction

ALL independent system operators (ISOs) in the US implement locational marginal cost pricing in which market participants pay or receive the cost of delivering the next unit of power at their node in the network. The marginal cost pricing approach is a cornerstone of ISO market design.

However, approximations within the market dispatch model differ from the network physics, and this causes problems in the market since prices do not reflect actual marginal costs [2], [3]. Making the modeling approximation as close as possible to the actual physics ensures that prices accurately reflect the marginal cost of electricity. This paper first derives an accurate linear loss function approximation from AC power flow, then proposes a novel method for updating the loss approximation without solving for a new AC-feasible base point.

The general name for the dispatch problem that ISOs solve is the optimal power flow (OPF). The AC Optimal Power Flow (ACOPF) accounts for alternating current's mathematical complexities. However, the ACOPF is a large scale, nonlinear, nonconvex optimization problem and requires more time to solve using existing methods than current practice in the day-ahead and real-time market (DAM and RTM) allows [4]. Dispatch models must solve quickly in order to be practical, which is why today's ISOs solve linear DCOPF model. The DCOPF does not model "direct current" power, but is a linearization and approximation of the ACOPF [5].

A. Current Practices

The magnitude of loss payments also justifies a closer look at current practices. In PJM in 2014, total marginal loss costs were \$1.5 billion, compared to \$1.9 billion in total congestion costs [6].

ISOs typically implement the DCOPF with power flow sensitivities called power transfer distribution factors (PTDFs) and line loss sensitivities called loss factors [7]. These sensitivities are linearized from a "base point" [5], which may be from a state estimator, AC power flow analysis, or dispatch solution.

The distribution factor model [7] requires the selection of a reference bus which is assumed to be the marginal source (or sink) of any changes in power consumed (or produced). Power flows to and from the reference bus are "summed" using the superposition principle, and therefore the effect of the reference bus cancels out in a lossless model. Although the reference bus simplifies the mathematics, its inclusion in the model can distort power flows when line losses are considered.

A common alternative to the distribution model approach is called the $B\Theta$ model [5], [8] and also results in a linear model. However, the $B\Theta$ model takes a few orders of magnitude longer to solve and therefore is not used to clear ISO markets. Therefore, this paper will focus on distribution factor implementations of the DCOPF, and in addition, will assume the use of the per-unit system. Table I provides a brief summary of the processes used by each ISO.

B. Literature Review

The DCOPF problem remains the standard problem for electric dispatch applications. Computational performance has always been the main advantage of using linear OPF models, as well as its easy integration with standard economic theory [9]. An early formulation and solution by Wells in 1968 reports solution times of a few minutes on power networks consisting of 100 nodes [10]. This work led to interest in more efficient DCOPF formulations and loss sensitivity calculations [5], [11]–[14]. In addition to computational advantages, the current formulations of the DCOPF show impressive–but not perfect–accuracy relative to AC power flows [15].

Various new approaches to the DCOPF remain an active area of research. One of the most important DCOPF applications is the calculation of locational marginal prices (LMPs) for electricity markets [7], [16]–[20]. The DCOPF is also an important aspect in transmission expansion planning [21], [22], renewable energy and storage integration [23], and other applications that are not enumerated here.

Iterative approaches to the DCOPF [16], [21], [24]–[27] have shown some success at improving the physical accuracy of the model. Some use additional AC power flow solutions after each iteration [16], [24], while others only use simplifications of the AC power flow equations [21], [25]–[27]. Line loss constraints for individual lines [26] or each node [27] can also improve the approximation, but results in a much larger model than using a single system-wide loss constraint [7].

However, the iterative approach has general advantages compared to methodologies that either require nonlinear solvers [28], or piecewise linearization through inequality constraints [26], [27] or binary variables [22]. While these approaches may have better accuracy, they also increase the model size. Other models use dispatch formulations that are not scalable for large networks, such as the $B\Theta$ power flow approximation [17] or current-based models [18].

C. Contributions

The key advantage of the proposed methodology is that it is based on the same DCOPF formulation used in current market software. Like standard practice, it linearizes the loss approximation directly from an initial AC power flow solution. The proposed approach is the only one in literature that uses an AC base point, can be updated without additional AC power flow solutions, and does not introduce any new variables or constraints that are not present in the standard model [7]. Additionally, the approach shows robust and accurate performance with a wide range of starting points.

The rest of the paper is organized as follows. Section II derives the DC power flow and loss approximations, and Section III formulates the linear DCOPF model. An example problem is presented in Section IV to compare the LMPs that result from three different DCOPF formulations. Section V

TABLE I
ISO LOSS FACTOR METHODOLOGIES

ISO	Used in Dispatch	Base Point (DAM)	Base Point (RTM)	Update Frequency
CAISO	Yes	AC power flow with generation and demand bids or load forecast	AC power flow with initial data from state estimator	Every hour in DAM and every fifteen minutes in RTM
ERCOT	No	Interpolation of on and off peak loss factors (during settlement process)	Interpolation of on and off peak loss factors (during settlement process)	N/A
ISO-NE	Yes	State estimator solution with estimated future operating conditions	Current state estimator solution	Every hour in DAM and every five minutes in RTM
MISO	Yes	Recent state estimator solutions with similar demand and wind characteristics	Current state estimator solution	Monitored in real time, with updates possible up to every minute
NYISO	Yes	AC power flow using a 30-day moving average of on and off peak power flows	AC power flow	During intermediate dispatch runs between DAM clearing and RTM clearing
PJM	Yes	State estimator solution with estimated future operating conditions	Current state estimator solution	Every hour in DAM and every five minutes in RTM
SPP	Yes	AC power flow with estimated future operating conditions	Current state estimator solution	Every hour in DAM and every five minutes in RTM

presents a method for updating loss factors and demonstrates the method on a selection of test cases. Section VI concludes the paper and is followed by references.

II. POWER FLOW DERIVATIONS

The purpose of this section is to formulate the traditional distribution factor model with losses and provide a method to accurately calculate marginal loss factors from a feasible AC power flow solution.

Using AC real power flow equations [4], power flows through branch $k \in \mathcal{K}$ can be defined from node i to j or from j to i,

$$p_{ijk} = g_k \frac{v_i^2}{a_{ijk}^2} - \frac{v_i v_j}{a_{ijk}}(g_k \cos(\theta_i - \theta_j - \phi_{ijk}) + b_k \sin(\theta_i - \theta_j - \phi_{ijk})), \ \forall k \in \mathcal{K} \quad (1)$$

$$p_{jik} = g_k v_j^2 - \frac{v_i v_j}{a_{ijk}}(g_k \cos(\theta_j - \theta_i + \phi_{ijk}) + b_k \sin(\theta_j - \theta_i + \phi_{ijk})), \ \forall k \in \mathcal{K} \quad (2)$$

where the parameters are the branch conductance g_k, branch susceptance b_k, tap transformer turns ratio a_{ijk}, transformer phase angle change ϕ_{ijk}, and the variables are the voltage magnitude v_i and voltage angle θ_i. Differences in p_{ijk} and p_{jik} will be used to calculate line losses, but otherwise it will be assumed that $p_{ijk} = -p_{jik}$. The real power flow variables are stored in a $K \times 1$ vector P_t.

The amount of power generated minus the amount consumed at a node must be equal to the amount flowing out of its adjacent transmission lines. Losses in the shunt conductance, g_i^{sh}, are also accounted for. For now, power generation (an injection) and consumption (a withdrawal) are simplified using the net injection p_i at node $i \in \mathcal{N}$, which by convention is positive for a net injection and negative for a net withdrawal. For real power, the network balance equations are

$$p_i = \sum_k p_{ijk} + v_i^2 g_i^{sh}, \ \forall i \in \mathcal{N}. \quad (3)$$

Or in matrix form,

$$P = \mathbf{A}^\top P_t + \mathbf{G_s}(V \circ V), \quad (4)$$

where $\mathbf{A}$ is a $K \times N$ network incidence equal to 1 if branch k is assumed to flow into node i, -1 if the branch is assumed to flow out of node i, and 0 if branch k is not connected to node i, $\mathbf{G_s}$ is an $N \times N$ diagonal matrix of shunt conductances, V is a vector of nodal voltage magnitudes, and $\circ$ is the element-by-element (or Hadamard) product.

A. DC Power Flow

Many industry applications rely on DC power flow approximations. DC power flow equations are preferable in many instances because they are linear and can be solved quickly. Conversely, AC power flow equations model the system more accurately, but are nonconvex. It can even be difficult to find a feasible solution to AC power flow equations in a large scale system such as one of the main US power grids. Therefore, the common DC power flow approximation makes three main assumptions:

1) Voltage is close to one per unit (p.u.) at all buses,
2) Voltage angle differences are small, i.e., $\sin(\theta_i - \theta_j) \approx \theta_i - \theta_j$ and $\cos(\theta_i - \theta_j) \approx 1$,
3) Line resistance is negligible compared to reactance, i.e., $r_k \ll x_k$ and therefore $g_k \ll b_k$.

Line conductance and susceptance are physical properties of the lines, and are respectively $g_k = \frac{r_k}{r_k^2 + x_k^2}$ and $b_k = \frac{-x_k}{r_k^2 + x_k^2}$. Under the assumptions above, (1) and (2) reduce to

$$P_t = -\mathbf{B_d}\left(\mathbf{A}\Theta + \Phi\right), \quad (5)$$

where $\mathbf{B_d}$ is a $K \times K$ diagonal matrix with values $b_k \approx \frac{-1}{x_k}$ for a lossless model, $\mathbf{A}$ is a $K \times N$ network incidence matrix, Θ is an $N \times 1$ vector of nodal voltage angles, and Φ is a $K \times 1$ vector of transformer phase angle changes.

To reduce solution time in practice, (5) can be simplified using power transfer distribution factors (PTDFs), also called shift factors [5]. PTDFs describe the fraction of real power injected at each bus that flows across each branch [29]. The injection

(or withdrawal) is assumed to be withdrawn (or injected) at the reference bus.

The PTDFs form a $K \times N$ sensitivity matrix $\mathbf{T}$ with elements $t_{(ijk,n)}$. Following similar derivations in references [29]–[31], an $N \times N$ nodal susceptance matrix is commonly defined,

$$\mathbf{B} = \mathbf{A}^\top \mathbf{B_d} \mathbf{A}. \tag{6}$$

Assuming $\Phi = 0$, combining (4), (5), and (6) gives,

$$P = \mathbf{B}\Theta. \tag{7}$$

Net injections P are replaced by a matrix of unit injections and reference bus withdrawals given by $[\mathbf{I} - W\mathbf{1}^\top]$, where W sums to one and defines the reference bus. Voltage angles Θ are then replaced by an $N \times N$ sensitivity matrix $\mathbf{H}$. The nth column of matrix $\mathbf{H}$ represents the marginal change in bus voltage angles corresponding to the net injections in the nth column of $[\mathbf{I} - W\mathbf{1}^\top]$,

$$[\mathbf{I} - W\mathbf{1}^\top] = \mathbf{BH}. \tag{8}$$

Combining (5) and (8) solves the PTDF matrix,

$$\mathbf{T} = -\mathbf{B_d}\mathbf{A}\mathbf{B}^{-1}[\mathbf{I} - W\mathbf{1}^\top]. \tag{9}$$

The matrix $\mathbf{B}$ is singular, so the row and column corresponding to the reference bus are removed to make it invertible. The matrix $[\mathbf{I} - W\mathbf{1}^\top]$ reduces to an identity matrix of size $N-1$ and can be omitted. The PTDF at the reference bus is zero by definition and assumes no line losses.

B. Marginal Line Losses

Loss factors define the linear sensitivity of total system losses to real power injections at each bus. Line losses are the sum of (1) and (2). Therefore, an $N \times N$ matrix $\mathbf{S}$ forms a set of marginal network balancing equations with the partial derivatives of p_{ijk} and p_{jik} with respect to voltage angles,

$$[\mathbf{S}]_{ij} = \begin{cases} \sum_{\mathcal{K}(i,j)} \frac{-\overline{v}_i \overline{v}_j}{a_{ijk}} \big(g_k \sin(\overline{\theta}_i - \overline{\theta}_j - \phi_{ijk}) \\ \quad - b_k \cos(\overline{\theta}_i - \overline{\theta}_j - \phi_{ijk})\big), & \text{if } i \sim j, \\ \sum_{\mathcal{K}(i)} \frac{\overline{v}_i \overline{v}_j}{a_{ijk}} \big(g_k \sin(\overline{\theta}_i - \overline{\theta}_j - \phi_{ijk}) \\ \quad - b_k \cos(\overline{\theta}_i - \overline{\theta}_j - \phi_{ijk})\big), & \text{if } i = j, \\ 0, & \text{otherwise.} \end{cases}$$

The change in voltage angles $\Delta\Theta$ resulting from a marginal real power injection ΔP is given by the linear system with a bordered matrix of $\mathbf{S}$ and the reference bus weights W,

$$\begin{bmatrix} \mathbf{S} & W \\ W^\top & 0 \end{bmatrix} \begin{bmatrix} \Delta\Theta \\ u \end{bmatrix} = \begin{bmatrix} \Delta P \\ 0 \end{bmatrix}. \tag{10}$$

The bottom row $W^\top \Delta\Theta = 0$ constrains the voltage angle at the reference bus, which is fixed at zero. The variable u is a reference bus withdrawal resulting from the marginal injections ΔP. The marginal loss is $1-u$, and therefore the loss factor is $\ell f_n = 1 - u$ if $\Delta p_n = 1$ and $\Delta p_i = 0$ for all $i \neq n$. Defining this system with unit injections at each bus creates a matrix inversion problem for the bordered matrix.

$$\begin{bmatrix} \mathbf{S} & W \\ W^\top & 0 \end{bmatrix} \begin{bmatrix} \mathbf{H_b} & \mathbf{1} \\ U^\top & 0 \end{bmatrix} = \mathbf{I}. \tag{11}$$

The loss factor vector is simply $LF = \mathbf{1} - U$. Loss factors for each branch can be computed by the solution for $\mathbf{H_b}$. Recall that line losses ℓ_k are given by the sum of (1) and (2).

$$\ell_k = g_k \left(\frac{v_i^2}{a_{ijk}^2} + v_j^2 - 2\frac{v_i v_j}{a_{ijk}} \cos(\theta_i - \theta_j - \phi_{ijk}) \right). \tag{12}$$

A $K \times N$ matrix $\mathbf{L}$ gives the partial derivatives $\partial \ell_k / \partial \theta_n$,

$$[\mathbf{L}]_{kn} = \begin{cases} 2g_k \frac{\overline{v}_i \overline{v}_j}{a_{ijk}} \sin(\overline{\theta}_i - \overline{\theta}_j - \phi_{ijk}), & \text{if } n = i, \\ -2g_k \frac{\overline{v}_i \overline{v}_j}{a_{ijk}} \sin(\overline{\theta}_i - \overline{\theta}_j - \phi_{ijk}), & \text{if } n = j, \\ 0, & \text{otherwise.} \end{cases} \tag{13}$$

Then a $K \times N$ matrix $\mathcal{L}$ with elements $\ell f_{kn} = \partial \ell_k / \partial p_n$ gives the loss factors for specific branches,

$$\mathcal{L} = \mathbf{L}\mathbf{H_b}. \tag{14}$$

It can be checked that $LF^\top = \mathbf{1}^\top \mathcal{L}$.

Lastly, a constant ℓ^0 is calculated such that the line loss approximation ℓ is exact at the base point,

$$\ell = \ell^0 + LF^\top (P_g - P_d). \tag{15}$$

Because (15) is linear, the constraint can be easily integrated into electricity market optimization software.

C. Alternative Line Loss Derivation

Alternatively, a set of loss factors can be derived using a common method ([8], [14], [19], [21], [22], [25]–[27]) which assumes that all voltages are equal to 1 p.u. and approximates $\cos\theta \approx 1 - \theta^2/2$. After some substitution, this yields a quadratic loss function,

$$\ell = \sum_k r_k p_{ijk}^2, \tag{16}$$

which leads to the following calculation for loss factors,

$$\ell f_n = 2 \sum_k r_k \overline{p}_{ijk} t_{(ijk,n)}, \ \forall n \in \mathcal{N}, \tag{17}$$

where ℓf_n is the nth element of the loss factor vector LF and $t_{(ijk,n)}$ is the PTDF for branch k and node n. This approximation loses some fidelity compared to (11) due to the assumption on voltages and the cosine approximation.

III. Model

The following analysis uses the DCOPF model proposed by a group at ISO-NE and ALSTOM EAI Corp. [7].

$$\min \quad c(P_g) \tag{18a}$$

$$\text{s.t.} \quad \mathbf{1}^\top (P_g - P_d) = \ell \tag{18b}$$

$$\ell = \ell^0 + LF^\top (P_g - P_d) \tag{18c}$$

$$-T_{\max} \le \mathbf{T}(P_g - P_d - D\ell) \le T_{\max} \tag{18d}$$

$$P_{\min} \le P_g \le P_{\max} \tag{18e}$$

where $c(\cdot)$ is a monotonically increasing cost function; the decision variables are power generation P_g and total system losses ℓ; parameters are power demand P_d, the loss function coefficients ℓ^0 and LF, loss distribution factors D, PTDFs $\mathbf{T}$, and physical limits $T_{\max}$, $P_{\min}$, and $P_{\max}$.

The loss distribution factor vector D is an $N \times 1$ vector that allocates line losses into nodal withdrawals. The short explanation is that (18d) needs to have the same amount of injections and withdrawals, but a more rigorous explanation is available in reference [7]. Following the example in [7], elements of D are proportional to the line losses in the branches connected to each bus.

LMPs are obtained by considering the dual problem of (18),

$$\max \lambda \mathbf{1}^\top P_d + \sigma \left(\ell^0 - LF^\top P_d\right) + \mu_{\max}^\top \left(T_{\max} + \mathbf{T} P_d\right) + \mu_{\min}^\top \left(T_{\max} - \mathbf{T} P_d\right) + {\alpha_{\min}}^\top P_{\min} - {\alpha_{\max}}^\top P_{\max} \tag{19a}$$

$$\text{s.t.} \ \lambda \mathbf{1} + \sigma LF + \mu_{\max}^\top \mathbf{T} - \mu_{\min}^\top \mathbf{T} + \alpha_{\min} - \alpha_{\max} = c \tag{19b}$$

$$\lambda + \sigma - \left(\mu_{\max} - \mu_{\min}\right)^\top \mathbf{T} D = 0 \tag{19c}$$

$$\mu, \alpha_{\min}, \alpha_{\max} \ge 0 \tag{19d}$$

Constraint (19b) forms the basis for LMPs, with the terms commonly decomposed into three components,

$$\lambda^E := \lambda \mathbf{1}, \tag{20}$$

$$\lambda^L := \sigma LF, \tag{21}$$

$$\lambda^C := \mu_{\max}^\top \mathbf{T} - \mu_{\min}^\top \mathbf{T}, \tag{22}$$

$$\Lambda := \lambda^E + \lambda^L + \lambda^C. \tag{23}$$

where λ^E, λ^L, and λ^C are the marginal costs of energy, losses, and congestion, all with respect to the reference bus.

IV. Model Comparison

This section will demonstrate the importance of initializing the OPF model with a good base point solution when clearing an electricity market. Three initializations of (18c) are tested:

1) DCOPF: ignore losses,
2) DCOPF-Q: loss function with marginal terms from (17),
3) DCOPF-L: loss function with marginal terms from (11).

Each initialization uses progressively more information from the base point solution. In this case, the base point is an ACOPF solution. The example is solved on the IEEE 300-bus network from the University of Washington test case archive [32], available in MATPOWER [33]. The analysis was implemented in GAMS based on code available from [34].

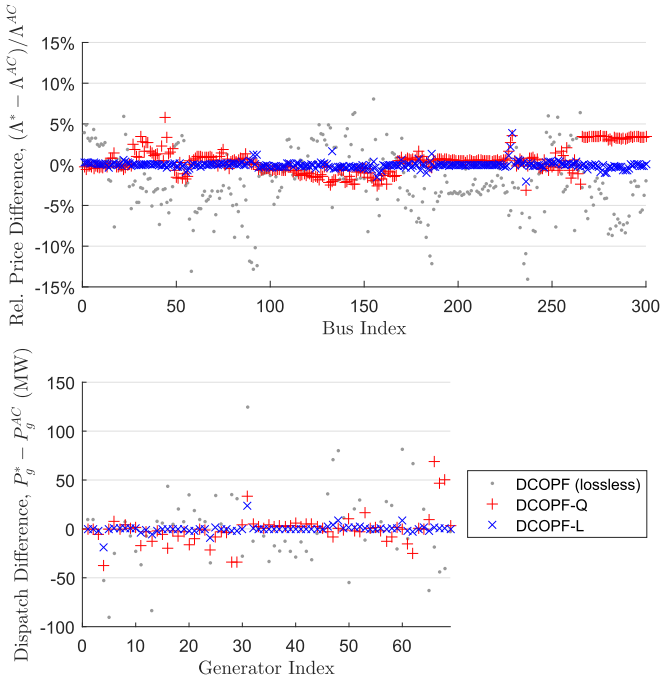

Fig. 1. Linear model LMPs and generator dispatch compared to ACOPF.

For the naive DCOPF model, the same model (18) can be initialized with $LF = \ell^0 = 0$. This inherent inaccuracy is compensated by proportionally increasing demand. That is, if there are ℓ^* losses in the base point solution, then the new demand parameters are, $\widetilde{P}_d := P_d \left(1 + \ell^* / \mathbf{1}^\top P_d\right)$. Of the other two models, DCOPF-Q is based on the quadratic approximation (16), which approximates the cosine function and assumes voltage is 1 p.u. whereas the DCOPF-L linearizes (12) without simplifying approximations.

Each of the three model initializations uses the same PTDFs. All other aspects of the model are held constant since the goal is to analyze the effect of model initializations on line loss estimation accuracy. Additionally, the network is not congested since we wish to discern aspects of the loss approximation independent of network congestion.

The linear model solutions are compared to solutions to an ACOPF model solved in GAMS [34]. The ACOPF is nonconvex, and may not always find the globally optimal solution. Nonetheless, it is used here as a benchmark for our DCOPF results. ACOPF LMPs are the dual variable of the real power balance constraint in an ACOPF solution [20], while DCOPF LMPs are calculated from (20)-(23).

A. LMP Accuracy

In the IEEE 300-bus example problem, prices from the ACOPF range from \$37.19/MWh to \$46.76/MWh. Considering that transmission losses are only 1.2% of total demand in this example, the total price spread may be surprising.

Fig. 1 shows that DCOPF-L is the most accurate model for pricing and dispatch. The most simplistic model, DCOPF, pro-

TABLE II
IEEE 300-BUS TEST CASE SOLUTION STATISTICS

Model	Avg. Disp. Diff. (MW)	LMP MAPE (%)	Rel. Cost Diff. (%)
DCOPF	25.9	3.77	−0.179
DCOPF-Q	9.3	1.23	−0.035
DCOPF-L	1.8	0.24	−0.002

duces only a single price for each node in the system. This causes inefficiencies because marginal losses are not considered, but it is included here to demonstrate a naive approach. The DCOPF-Q model does a better job of differentiating locations based on marginal losses, but it also mis-estimates the marginal effect by a large amount at some buses because it assumes network voltages are at their nominal values. The DCOPF-L produces prices and dispatch that are very similar to the ACOPF, the closest of all three linear models.

Looking at the maximum LMP error in the network, DCOPF underestimates the LMP at bus 528 by 14.1%, DCOPF-Q overestimates at bus 51 by 5.7%, and DCOPF-L overestimates at bus 250 by 3.8%. Further comparisons of the three models are given in Table II. Three summary statistics are defined by,

$$\text{Avg. Dispatch Diff.} = \frac{1}{N}\sum_i \left| p_i^{g*} - p_i^{g,AC} \right|, \tag{24}$$

$$\text{LMP MAPE} = \frac{1}{N}\sum_i \frac{\left|\Lambda_i^* - \Lambda_i^{AC}\right|}{\Lambda_i^{AC}} \times 100\%, \tag{25}$$

$$\text{Rel. Cost Diff.} = \frac{c(P_g^*) - c(P_g^{AC})}{c(P_g^{AC})} \times 100\%. \tag{26}$$

The relative performance of the three models is network-specific, but in most cases, the three models will either perform similarly or the DCOPF-L will perform significantly better because it can be tuned to the current operating conditions of the network. Higher voltages generally translate to lower line losses. The DCOPF-Q model assumes voltages are at their nominal levels and consequently overestimates marginal losses where the network is operating at higher than its nominal voltage (shown in Fig. 1 at bus indices 265-300). The DCOPF-L computes losses with respect to the base point voltage magnitude and voltage angle, so its loss factors reflect voltages that are different than nominal values.

It should be emphasized that improved loss function accuracy leads to better prices and dispatch without any additional computational cost. On the IEEE 300-bus test case, the DCOPF-L initialization decreases the relative cost difference with the ACOPF by more than twentyfold compared to DCOPF-Q and one-hundredfold compared to the naive DCOPF model. Average dispatch difference and LMP MAPE are both reduced by about fivefold compared to DCOPF-Q and fifteenfold compared to DCOPF.

The next section updates the loss approximation using the real power flow p_{ijk}^* in the optimal solution of DCOPF-L.

TABLE III
TWO NODE EXAMPLE

Generators				
	Bus	Initial Bid ($)	Final Bid ($)	Capacity (MW)
A	1	30.00	29.50	10
B	1	30.00	29.75	100
C	2	30.00	30.00	100
Transmission			Load	
From	To	Resistance (Ω)	Bus	Demand (MW)
1	2	0.0005	2	90

TABLE IV
SOLUTIONS FOR INITIAL AND FINAL BIDS

	Solution		
Dispatch	1	2	3
Gen A	10 MW	10 MW	0 MW
Gen B	84.46 MW	0 MW	0 MW
Gen C	0 MW	80.05 MW	90 MW
Flow	94.46 MW	10 MW	0 MW
Losses	4.46 MW	0.05 MW	0 MW
Initial Cost	$2,833.84	$2,701.50	$2,700.00
Final Cost	$2,807.73	$2,696.50	$2,700.00

V. QUADRATIC UPDATE PROCEDURE

A. Motivating Example

The base point in the previous section was the ACOPF solution, but such a good base point is not possible in practice. The following motivating example shows how a suboptimal base point can lead to inefficient dispatch.

Consider the two node problem described in Table III. Three generators initially have identical costs and are connected by a lossy transmission line. For simplicity, it is assumed that the voltage at both nodes is 1, so line losses are equal to $r_{12}(p_{12})^2$.

A few potential solutions are given in Table IV. Solution 3 is clearly optimal for the initial bids, and the dispatch cost is given on the 'Initial Cost' line. Suppose that in the next time period, generators A and B reduce their bids after purchasing new gas contracts on the spot market. Instead of $30, the new bids are $29.50 for generator A and $29.75 for generator B. The new costs are shown on the 'Final Cost' line of Table IV, and Solution 2 is optimal.

However, there is a key point that current practices miss in this scenario! Suppose that Solution 3 is used as a base point to calculate loss factors. There are no losses in the network since $p_{12} = 0$, so loss factors at both nodes are zero. Therefore the dispatch model would select the cheapest generators, A and B, corresponding to Solution 1. If the model were given an accurate set of loss factors then it would have selected Solution 2, so the actual dispatch will cost almost 4% more than the optimal solution.

B. Algorithm Description

This section proposes a sequential linear programming (SLP) method to update loss factors in such a case. This results in a more accurate representation of marginal losses, which results in more accurate prices and more efficient dispatch.

The core idea in the SLP methodology comes from Section II-C and the fact that $\ell = \sum_k r_k p_{ijk}^2$ gives a decent approximation for line losses. When linearized, this function splits into linear terms ($2r_k\overline{p}_{ijk}t_{(ijk,n)}$) analogous to ℓf_n and some constant terms ($r_k\overline{p}_{ijk}^2$) analogous to ℓ^0. Each time the model is solved, the line loss function can be updated with new values p_{ijk}^*. If $p_{ijk}^* = \overline{p}_{ijk}$, then the optimal solution is the same as the base point solution and the model has a good representation of marginal line losses. Section IV shows that the quadratic approximation (17) can result in significant pricing errors, so the SLP algorithm combines the quadratic approach with the more accurate loss factor initialization using (11).

Loss functions for each branch can be computed individually and then summed to represent total system losses. The loss functions will take a quadratic form similar to (16),

$$\ell = \sum_k \ell_k = \sum_k \left(\gamma_k(p_{ijk} + \xi_k)^2 + \eta_k\right). \tag{27}$$

Any quadratic function can be given by different values of γ_k, ξ_k and η_k, so (27) can be assumed without loss of generality. Unfortunately, the initial loss function does not provide enough information to calculate all three of these coefficients, so the following is derived from (12),

$$\frac{d\ell_k}{dp_n} = \frac{d\ell_k}{d\theta}\frac{d\theta}{dp_n} \approx 2r_k\frac{\overline{v}_i\overline{v}_j}{a_{ijk}}\overline{p}_{ijk}t_{(ijk,n)}. \tag{28}$$

Based on this, let $\gamma_k = r_k\frac{\overline{v}_i\overline{v}_j}{a_{ijk}}$. Rearranging the first order Taylor series of (27) gives,

$$\ell_k \approx 2\gamma_k(\overline{p}_{ijk} + \xi_k)p_{ijk} + \gamma_k(\xi_k^2 - \overline{p}_{ijk}^2) + \eta_k. \tag{29}$$

Define ℓf_{kn}, ℓ_k^0, ℓf_n and ℓ^0 so that the approximation is in the same terms as (15),

$$\ell f_{kn} := 2\gamma_k(\overline{p}_{ijk} + \xi_k)t_{(ijk,n)}, \tag{30}$$

$$\ell_k^0 := \gamma_k(\xi_k^2 - \overline{p}_{ijk}^2) + \eta_k, \tag{31}$$

$$\ell f_n := \sum_k \ell f_{kn}, \tag{32}$$

$$\ell^0 := \sum_k \ell_k^0. \tag{33}$$

The initial ℓf_{kn} and ℓ_k^0 determine the coefficients ξ_k and η_k,

$$\xi_k = \frac{\ell f_{kn}}{2\gamma_k t_{(ijk,n)}} - \overline{p}_{ijk}, \tag{34}$$

$$\eta_k = \ell_k^0 - \gamma_k(\xi_k^2 - \overline{p}_{ijk}^2). \tag{35}$$

The loss function is a first order Taylor series approximation of (27) and can be updated with new values $\overline{p}_{ijk}$. If an initial AC solution is not available, one can assume $\gamma_k = r_k$ and $\xi_k = \eta_k = 0$, and the algorithm is the essentially same as the SLP described in [21]. The general algorithm is shown in Fig. 2, with the following few numerical side notes.

Require: $t_{(ijk,n)}, d_n, r_k, a_{ijk}, \ell f_i, \ell^0, \overline{p}_n^g, \overline{p}_n^d, \overline{\ell}, \overline{v}_i$

1: $\overline{p}_{ijk} \leftarrow \sum_n t_{(ijk,n)}(\overline{p}_n^g - \overline{p}_n^d - d_n\overline{\ell})$ $\{\forall k \in \mathcal{K}\}$
2: $\gamma_k \leftarrow r_k\overline{v}_i\overline{v}_j/a_{ijk}$ $\{\forall k \in \mathcal{K}\}$
3: $\xi_k \leftarrow \ell f_{kn}/2\gamma_k t_{(ijk,n)} - \overline{p}_{ijk}$ $\{\forall k \in \mathcal{K}$
$n = \arg\max_m(|t_{(ijk,m)}| : m \in \{i,j\})\}$
4: $\eta_k \leftarrow \ell_k^0 - \gamma_k(\xi_k^2 - \overline{p}_{ijk}^2)$ $\{\forall k \in \mathcal{K}\}$
5: **solve** (18), $h = 1$
6: **while** $\frac{|c(P_g^h) - c(P_g^{h-1})|}{c(P_g^{h-1})} \geq tol$ and $h \leq h^{\max}$ **do**
7: $\overline{p}_n^g \leftarrow p_n^{g*}, \overline{p}_{ijk} \leftarrow p_{ijk}^*$ $\{\forall n \in \mathcal{N}, \forall k \in \mathcal{K}\}$
8: $\overline{\ell} \leftarrow \sum_k \gamma_k(\overline{p}_{ijk} + \xi_k)^2 + \eta_k$
9: $\ell f_n \leftarrow 2\sum_k \gamma_k(\overline{p}_{ijk} + \xi_k)t_{(ijk,n)}$ $\{\forall n \in \mathcal{N}\}$
10: $\ell^0 \leftarrow \overline{\ell} - \sum_n \ell f_n(\overline{p}_n^g - p_n^d)$
11: **solve** (18), $h \leftarrow h + 1$
12: **end while**

Fig. 2. Pseudocode for loss function SLP.

The assignment of ξ_k requires an arbitrary selection for the index n for ℓf_{kn} and $t_{(ijk,n)}$. This can be a source of numerical errors, but choosing $n = \arg\max_m(|t_{(ijk,m)}| : m \in \{i,j\})$ helps to minimize these errors. Another numerical issue can occur when calculating ξ_k if γ_k is very small or zero due to very low resistance on the line. In this case, set a tolerance value ε_γ and let $\xi_k = \gamma_k = 0$ if $\gamma_k < \varepsilon_\gamma$.

In Line 6 of the algorithm in Fig. 2, any convergence criterion can be set that fits operational needs. The algorithm is shown with criteria on the relative change in objective function and an iteration limit $h^{\max}$, but there are many other options.

Lastly, the update rule can be amended using a damping parameter $\omega \in [0, 1]$ in Line 7 of the algorithm,

$$\overline{p}_n^{g,h+1} = \omega\overline{p}_n^{g,h} + (1-\omega)p_n^{g*}, \tag{36}$$

$$\overline{p}_{ijk}^{h+1} = \omega\overline{p}_{ijk}^{h} + (1-\omega)p_{ijk}^{*}. \tag{37}$$

Each iteration in this SLP solves an approximation of a quadratically constrained program (QCP). This QCP is the same formulation as (18) except that the constraint (18c) is replaced with (27). The problem is non-convex since this constraint is an equality instead of a greater-than-or-equal-to constraint, so a locally optimal solution is not guaranteed to be the globally optimal solution. The following relaxation of (27) is solved so that converged solution of the SLP can be compared with the global optimum of the QCP,

$$\ell \geq \sum_k \left(\gamma_k(p_{ijk} + \xi_k)^2 + \eta_k\right). \tag{38}$$

This relaxation makes the problem convex, and therefore any locally optimal solution is also a globally optimal solution. Introducing inequality loss constraints may cause "artificial losses" when the constraint is not binding. The loss constraint was binding in each solution of the relaxed problem, and therefore the relaxed solutions were also optimal in the unrelaxed QCP.

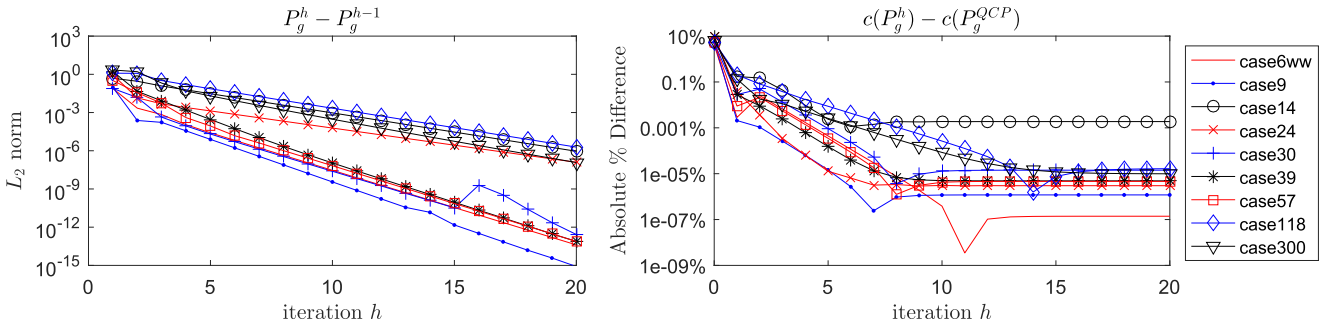

Fig. 3. Convergence with respect to the change in generator dispatch (left) and with respect to the cost of the optimal QCP (right).

C. Convergence Results

Results for implementing the algorithm are shown in Fig. 2 on a selection of test cases from the University of Washington test case archive [32] as well as few other that are available in MATPOWER [33]. The analysis was implemented in GAMS based on code available from [34].

Including the damping parameter ω improved the convergence speed of all test cases, and the 118- and 300-bus cases did not converge unless the damping parameter was used. After some trial and error, $\omega = 0.25$ for the smaller cases ($<$100 buses) and $\omega = 0.5$ for the larger cases (118- and 300-bus networks) showed good results. Generally, setting ω too large can slow down convergence, but setting it too small may lead it to diverge.

The results in Fig. 3 were obtained by uniformly increasing demand parameters by 5% compared to the base point solution and randomizing generator costs by multiplying by a normal random variable, $N(1, 0.02)$. The randomization step was necessary because many of the generators have identical cost functions in the original data sets. These parameter changes led to a binding line limit in the 39-bus network, but did not affect convergence.

Convergence was measured with the standard L_2 norm, defined as the square root of the sum of squared differences. Each iterative solution to (18) is indexed by h. Values for P_g^h, P_t^h and Λ^h were compared with the previous iteration. Results were similar for each of P_g^h, P_t^h and Λ^h, so only P_g^h is shown to save space. Fig. 3 also shows convergence with respect to the objective function of the QCP.

As shown in Fig. 3, all objective functions appear to converge within 0.01% of the QCP solution by the sixth iteration in each test case. Although there is no guarantee for convergence, it was fairly easy to achieve the results using a very simple damping method. Step size constraints may also be useful in larger or more complex networks, but their use was unnecessary in these test cases.

Results of the SLP were compared with the QCP and ACOPF. Table V provides the number of iterations for the SLP to converge, and the Avg. Dispatch Diff., LMP MAPE, and Rel. Cost Diff. of the SLP with respect to the ACOPF solution. Convergence criteria was met if the change in objective value function was less than 0.01% between iterations. All test cases met this criteria within two or three iterations.

TABLE V
SOLUTION COMPARISON OF SLP AND ACOPF

Network	Avg. Disp. Diff. (MW)	LMP MAPE (%)	Rel. Cost Diff. (%)
case6ww	0.121	0.725	−0.135
case9	0.006	0.375	−0.007
case14	0.163	0.270	−0.379
case24	0.125	0.406	0.041
case30	0.035	0.393	−0.129
case39	3.551	1.246	0.039
case57	3.575	1.239	−0.094
case118	0.983	0.255	−0.229
case300	6.223	0.912	−0.023

TABLE VI
COMPUTATIONAL COMPARISON OF SLP, QCP, AND ACOPF

Network	SLP	Solution time* (s)		
	Iterations	SLP	QCP	ACOPF
case6ww	2	0.026	0.177	0.171
case9	3	0.053	0.167	0.295
case14	2	0.042	0.167	0.285
case24	3	0.072	0.241	0.378
case30	2	0.070	0.260	0.264
case39	3	0.059	0.232	0.273
case57	2	0.068	0.235	0.373
case118	2	0.117	0.458	0.635
case300	2	0.246	0.625	1.157

*average of ten trials

Table VI compares solution times of the three models. Analytical bounds between the SLP and ACOPF solutions would be difficult or impossible to prove, but the SLP model converges within 0.4% of a locally optimal ACOPF solution for each of the cases tested. Approximating the ACOPF with the SLP requires only a fraction of the solution time.

Solution times were measured on a laptop computer with a 2.30 GHz processor and 8GB of RAM. CPLEX 12.5 solved SLP and Ipopt solved the QCP and ACOPF. PTDF values less than 0.01 were removed and quadratic cost functions were approximated as piecewise linear functions with ten steps to improve solution times. Both techniques have a minimal change in the dispatch solution.

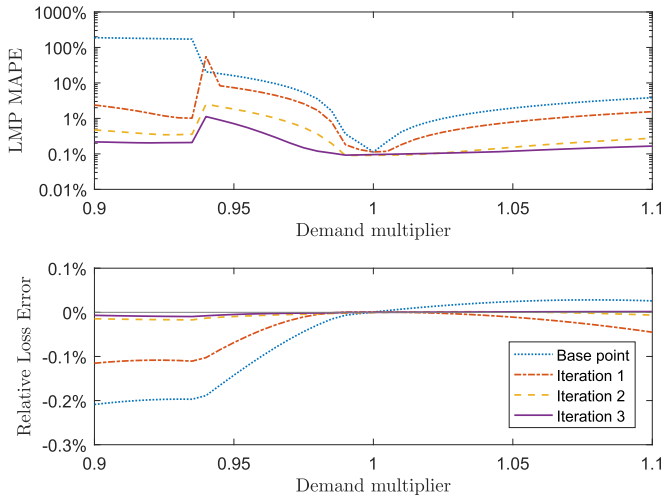

Fig. 4. Effect of changes in demand on the accuracy of LMPs (top) and the loss approximation (bottom) with respect to local ACOPF solutions in the IEEE 24-bus network [32].

D. Sensitivity Results

Performing a sensitivity analysis on the entire suite of network cases [32] illustrated the SLP's dependence on a good starting point. The 24-bus network tended to have a poor base point, and its results are shown in detail in Fig. 4. The sensitivity is performed by scaling demand by uniform factors ranging from 0.90 to 1.10 in 0.01 increments. At each step in the sensitivity, the base point solution is the same and is updated according to the algorithm in Fig. 2 with a damping parameter $\omega = 0.25$ (and $\omega = 0.5$ for the 118- and 300-bus networks).

The sensitivity analysis measured the effect of increased demand on accuracy of the LMP and the loss approximation with respect to marginal prices and losses calculated by a nonlinear ACOPF problem [34]. LMP accuracy is again measured by MAPE, and loss accuracy was measured by relative error,

$$\text{Relative Loss Error} = \frac{\ell^* - \ell^{AC}}{\ell^{AC}} \times 100\%. \qquad (39)$$

As illustrated with the sensitivity analysis, the proposed approach is fairly robust to non-ideal starting points. Across all networks and all sensitivities, the average LMP MAPE at Iteration 3 was 0.95% (worst-case 3.07% in the 39-bus network) and the average relative loss error was 0.02% (worst-case 0.42% in the 14-bus network). These results were obtained by selecting a relatively naive damping rule, and may possibly be improved by choosing a more sophisticated update rule or introducing step-size constraints between iterations.

VI. Conclusion

The DCOPF is at the core of many applications in today's electricity markets. Computational advantages of its LP formulation come at the expense of approximating the physics of power flow. The analysis presented in this paper therefore focuses on improving DCOPF accuracy while keeping the LP structure. Practical implementation of the SLP algorithm in an ISO-scale network would be an important step in proving its computational effectiveness, which is left for future work.

Additionally, the proposed approach motivates a broader analysis of trade-offs between computation speed and physical accuracy of dispatch models. For example, speed requirements or the availability of a base-point solution may be different in real time dispatch or long-term planning contexts. Various approximation methods, such as piecewise linear approximations [26], [27] or quadratic programming [28], should be compared in each context.

Accuracy of the loss approximation should not be ignored. A feasible AC base point provides valuable information about voltage angles and voltage magnitudes that are omitted from traditional DCOPF formulations. Adding this information improves the accuracy of marginal line losses.

The analysis presented in this paper can be of use to many researchers and practitioners interested in modeling electricity markets. Inaccuracy of the dispatch model's marginal terms significantly affects generator dispatch and remuneration. The methods explained in this paper help to reduce this inaccuracy.

References

[1] B. Eldridge, R. P. O'Neill, and A. Castillo, *Marginal Loss Calculations for the DCOPF*, Federal Energy Regulatory Commission, Washington, DC, USA, Jan. 2017.

[2] *2011 State of the Market Report for the MISO Electricity Markets*, Potomac Economics, Fairfax, VA, USA, Jun. 2012.

[3] *Order Assessing Civil Penalties IN15-3-000*, Federal Energy Regulatory Commission, Washington, DC, USA, May 2015.

[4] M. B. Cain, R. P. O'Neill, and A. Castillo, "*Optimal Power Flow Papers and Formulations*, Federal Energy Regulatory Commission, Washington, DC, USA, Jul. 2015.

[5] B. Stott, J. Jardim, and O. Alsaç, "DC power flow revisited," *IEEE Trans. Power Syst.*, vol. 24, no. 3, pp. 1290–1300, Aug. 2009.

[6] *State of the Market Report for PJM: Section 11 Congestion and Marginal Losses*, Monitoring Analytics, LLC, Eagleville, PA, USA, Mar. 2015.

[7] E. Litvinov, T. Zheng, G. Rosenwald, and P. Shamsollahi, "Marginal loss modeling in LMP calculation," *IEEE Trans. Power Syst.*, vol. 19, no. 2, pp. 880–888, May 2004.

[8] F. C. Schweppe, M. C. Caramanis, R. D. Tabors, and R. E. Bohn, *Spot Pricing of Electricity*. Norwell, MA, USA: Kluwer, 1988.

[9] M. C. Caramanis, R. E. Bohn, and F. C. Schweppe, "Optimal spot pricing: practice and theory," *IEEE Trans. Power App. Syst.*, vol. PAS-2, no. 9, pp. 3234–3245, Sep. 1982.

[10] D. Wells, "Method for economic secure loading of a power system," *Proc. Inst. Electr. Eng.*, vol. 115, no. 8, pp. 1190–1194, 1968.

[11] B. Stott and J. Marinho, "Linear programming for power-system network security applications," *IEEE Trans. Power App. Syst.*, vol. PAS-3, no. 98, pp. 837–848, May 1979.

[12] R. R. Shoults, W. M. Grady, and S. Helmick, "An efficient method for computing loss formula coefficients based upon the method of least squares," *IEEE Trans. Power App. Syst.*, vol. PAS-98, no. 6, pp. 2144–2152, Nov. 1979.

[13] O. Alsac, J. Bright, M. Prais, and B. Stott, "Further developments in LP-based optimal power flow," *IEEE Trans. Power Syst.*, vol. 5, no. 3, pp. 697–711, Aug. 1990.

[14] Y.-C. Chang, W.-T. Yang, and C.-C. Liu, "A new method for calculating loss coefficients [of power systems]," *IEEE Trans. Power Syst.*, vol. 9, no. 3, pp. 1665–1671, Aug. 1994.

[15] T. J. Overbye, X. Cheng, and Y. Sun, "A comparison of the AC and DC power flow models for LMP calculations," in *Proc. IEEE 2004 37th Annu. Hawaii Int. Conf. Syst. Sci*, 2004.

[16] Z. Hu, H. Cheng, Z. Yan, and F. Li, "An iterative LMP calculation method considering loss distributions," *IEEE Trans. Power Syst.*, vol. 25, no. 3, pp. 1469–1477, Aug. 2010.

[17] T. Orfanogianni and G. Gross, "A general formulation for LMP evaluation," *IEEE Trans. Power Syst.*, vol. 22, no. 3, pp. 1163–1173, Aug. 2007.
[18] J.-C. Peng, H. Jiang, G. Xu, A. Luo, and C. Huang, "Independent marginal losses with application to locational marginal price calculation," *IET Gener., Transmiss. Distrib.*, vol. 3, no. 7, pp. 679–689, 2009.
[19] F. Li, "Fully reference-independent LMP decomposition using reference-independent loss factors," *Elect. Power Syst. Res.*, vol. 81, no. 11, pp. 1995–2004, 2011.
[20] H. Liu, L. Tesfatsion, and A. Chowdhury, "Locational marginal pricing basics for restructured wholesale power markets," in *Proc. 2009 IEEE Power Energy Soc. General Meeting*, 2009, pp. 1–8.
[21] B. F. Hobbs, G. Drayton, E. B. Fisher, and W. Lise, "Improved transmission representations in oligopolistic market models: Quadratic losses, phase shifters, and DC lines," *IEEE Trans. Power Syst.*, vol. 23, no. 3, pp. 1018–1029, Aug. 2008.
[22] D. Z. Fitiwi, L. Olmos, M. Rivier, F. de Cuadra, and I. Pérez-Arriaga, "Finding a representative network losses model for large-scale transmission expansion planning with renewable energy sources," *Energy*, vol. 101, pp. 343–358, 2016.
[23] A. Castillo, X. Jiang, and D. Gayme, "Lossy DCOPF for optimizing congested grids with renewable energy and storage," in *Proc. IEEE 2014 Amer. Control Conf.*, 2014, pp. 4342–4347.
[24] F. Li and R. Bo, "DCOPF-based LMP simulation: Algorithm, comparison with ACOPF, and sensitivity," *IEEE Trans. Power Syst.*, vol. 22, no. 4, pp. 1475–1485, Nov. 2007.
[25] V. N. Bharatwaj, A. Abhyankar, and P. Bijwe, "Iterative DCOPF model using distributed slack bus," in *Proc. 2012 IEEE Power Energy Soc. General Meeting*, 2012, pp. 1–7.
[26] T. N. D. Santos and A. L. Diniz, "A dynamic piecewise linear model for dc transmission losses in optimal scheduling problems," *IEEE Trans. Power Syst.*, vol. 26, no. 2, pp. 508–519, May 2011.
[27] A. Helseth, "A linear optimal power flow model considering nodal distribution of losses," in *Proc. 2012 IEEE 9th Int. Conf. Eur. Energy Market*, 2012, pp. 1–8.
[28] R. A. Jabr, "Modeling network losses using quadratic cones," *IEEE Trans. Power Syst.*, vol. 20, no. 1, pp. 505–506, Feb. 2005.
[29] A. J. Wood, B. F. Wollenberg, and G. B. Sheblé, *Power Generation, Operation and Control*. Hoboken, NJ, USA: Wiley, 2013.
[30] X. Cheng and T. J. Overbye, "PTDF-based power system equivalents," *IEEE Trans. Power Syst.*, vol. 20, no. 4, pp. 1868–1876, Nov. 2005.
[31] H. Ronellenfitsch, D. Manik, J. Horsch, T. Brown, and D. Witthaut, "Dual theory of transmission line outages," *IEEE Trans. Power Syst.*, vol. 32, no. 5, pp. 4060–4068, Sep. 2017.
[32] "Power systems test case archive," Univ. Washington, Seattle, WA, USA, Tech. Rep., 1999. [Online]. Available: http://www2.ee.washington.edu/research/pstca
[33] R. D. Zimmerman, C. E. Murillo-Sánchez, and R. J. Thomas, "MATPOWER: Steady-state operations, planning and analysis tools for power systems research and education," *IEEE Trans. Power Syst.*, vol. 26, no. 1, pp. 12–19, Feb. 2011.
[34] L. Tang and M. Ferris, "Collection of power flow models: Mathematical formulations," 2015. [Online]. Available: http://www.neos-guide.org/sites/default/files/math_formulation.pdf

Brent Eldridge received the B.S. degree in industrial engineering from Texas A&M University, College Station, TX, USA, in 2011 and the M.S. degree in industrial engineering and operations research from the University of California, Berkeley, CA, USA, in 2014. He is currently working toward the Ph.D. degree at Johns Hopkins University, Baltimore, MD, USA. His current research interests are in mathematical optimization and the economics of electricity markets.

Richard O'Neill received the B.S. degree in chemical engineering and the Ph.D. degree in operations research both from the University of Maryland at College Park. Currently, he is the Chief Economic Advisor in the Federal Energy Regulatory Commission (FERC), Washington, DC, USA. He was previously on the faculty of the Department of Computer Science, Louisiana State University, Baton Rouge, and the Business School at the University of Maryland at College Park.

Anya Castillo received the B.S. degree in electrical and computer engineering from Carnegie Mellon University, Pittsburgh, PA, USA, the M.S. degree from Engineering Systems Division, Massachusetts Institute of Technology, Cambridge, MA, USA, and the Ph.D. degree in environmental engineering from Johns Hopkins University, Baltimore, MD, USA. She is currently a Senior Member of Technical Staff with Sandia National Laboratories, Albuquerque, NM, USA.